Application of Active Controls Technology to Aircraft Ride Smoothing

Ira D. Jacobson* and Maris Lapins†
University of Virginia, Charlottesville, Va.

Prototype ride smoothing systems (RSS's) were synthesized for flight testing aboard the NASA general purpose airborne simulator (GPAS). The systems were designed to meet comprehensive criteria, including passenger comfort and aircraft handling qualities considerations. System performance estimates based on analytic expressions were compared to estimates derived from digital calculations. The effects of RSS's on pilot workload during instrument landing system (ILS) approach in turbulence was examined in a fixed-base simulator. A limited number of flights were conducted to verify predicted RSS performance. Results of these experiments indicate that the RSS's reduce pilot workload and increase passenger comfort, while maintaining handling qualities.

Nomenclature

a_x = longitudinal acceleration along the x-body axis at the center of gravity (positive forward)
a_y = lateral acceleration along the y-body axis at the center of gravity (positive out right wing)
a_z = normal acceleration along the z-body axis at the center of gravity (positive down)
C_j = comfort rating [Eq. (1)]
G_i = transfer function of output j due to input i
$j\omega$ = imaginary part of complex variable, $s=\sigma\pm j\omega$
K_i = feedback gain particularized by subscript
L = rolling moment about the x axis due to aerodynamic torques (positive right wing down)
M = pitching moment about the y axis due to aerodynamic torques (positive nose up)
n/α = handling qualities parameter
N = yawing moment about z axis due to aerodynamic torques (positive nose right)
p = roll rate; angular velocity about x axis (positive right wing down)
q = pitch rate; angular velocity about y axis (positive nose up)
r = yaw rate; angular velocity about z axis (positive nose right)
s = Laplace operator, $\sigma+j\omega$
$T_{1/2}$ = time to ½ amplitude
T_2 = time to double amplitude
U_0 = linear steady-state velocity along the x axis (positive forward)
v = linear perturbed velocity along the y axis (positive out right wing)
V_{T_0} = total linear steady-state velocity (positive forward)
w = linear perturbed velocity along the z axis (positive down)
Y = aerodynamic force along the y axis (positive out right wing)
Z = aerodynamic force along the z axis (positive down)
β = sideslip angle
δ_f = direct lift flap deflection (positive for trailing edge down)
δ_e = elevator surface deflection from trim (positive for nose down pitching moment for aft surface)
δ_r = rudder deflection (positive for nose-left yawing moment (negative N))
δ_{sfg} = side force generator deflection (positive for trailing edge left)
ζ_i = damping ratio of linear second-order mode particularized by subscript
Λ = white noise
θ = perturbation pitch angle (positive nose up)
θ_0 = steady-state (trim) pitch angle
σ = real portion of complex variable, $s=\sigma\pm j\omega$
σ_i = root-mean-square intensity of motion quantity, forcing function, or surface deflection particularized by subscript
τ_i = time constant of first-order mode particularized by subscript
$\Phi(i)$ = power spectral density of quantity (i)
ω = spectral frequency
ω_{n_i} = undamped natural frequency of second-order mode particularized by subscript

Subscripts

c = control surface actuator command
dr = Dutch roll mode
g = gust
ph = phugoid mode
R = roll subsidence mode
s = spiral mode
sp = short-period mode
st = static

Received Aug. 1, 1975; presented as Paper 75-1029 at the AIAA 1975 Aircraft Systems and Technology Meeting, Los Angeles, Calif., Aug. 4-7, 1975; revision received April 13, 1977.

Index categories: Handling Qualities, Stability and Control; Testing, Flight and Ground.

*Associate Professor, Department of Engineering Science and Systems, School of Engineering and Applied Science. Member AIAA.

†Graduate Research Assistant, Department of Engineering Science and Systems, School of Engineering and Applied Science. Student Member AIAA.

I. Introduction

THE problem of providing smooth flight in the presence of atmospheric turbulence has been studied periodically by numerous investigators over the past 70 years; the sophistication of proposed solutions is increasing as new analytical tools and hardware become available. Recently, little attention has been devoted to the subject because of the relative insensitivity of contemporary aircraft to gust upset. With the advent of short takeoff and landing (STOL) aircraft, in particular low wing loading STOL, passenger comfort and structural weight considerations have sparked renewed interest in active control of gust loads.

The purpose of this paper is to report on a recent analytical and experimental study of ride smoothing systems (RSS's)

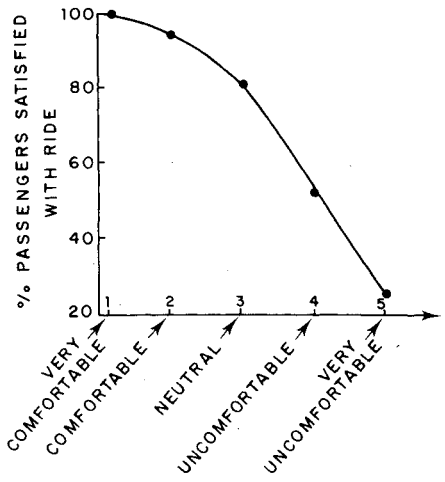

Fig. 1 Passenger satisfaction criteria.

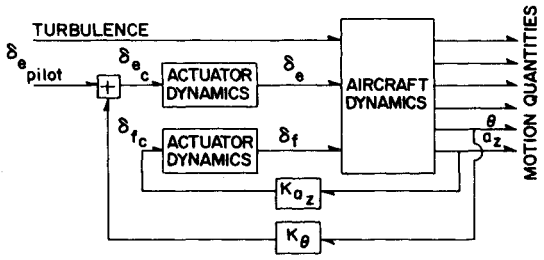

Fig. 2 Basic longitudinal ride smoothing system.

designed for STOL-class aircraft. This study differs from previous investigations in several important aspects. First, multiple-feedback, closed-loop RSS's were designed to suppress turbulence-induced motion in both the longitudinal and lateral axes. The essential feedbacks were acceleration measured at the center of gravity (a_z and a_y), and the primary control surfaces were direct lift flaps and direct side force generators. Second, a comprehensive set of RSS design criteria, intended to include the requirements of all components of the aircraft/pilot/passenger system, were established. Specifically, RSS effectiveness with respect to passenger comfort was determined from the University of Virginia comfort model for motion dominated by vertical acceleration,[1] which relates subjective comfort C to rms vertical σ_{a_z} and lateral σ_{a_y} accelerations as follows:

$$C = 2 + 11.9\sigma_{a_z} + 7.6\sigma_{a_y} \tag{1}$$

For this model, the scale associated with comfort is given as: $C=1$ – very comfortable; $C=2$ – comfortable; $C=3$ – neutral; $C=4$ – uncomfortable; $C=5$ – very uncomfortable. (Since the model is empirically determined, and passengers do not use the end-point of the scale, the constant is greater than 1.) These subjective passenger reactions have been correlated to passenger satisfaction with ride quality as shown in Fig. 1. The requirements of MIL-F-8785B[2] for level 1 (acceptable) handling qualities for class II-L (land-based medium transports) in category C (terminal) flight phase were used to determine desirable locations of closed-loop system characteristic roots. Furthermore, adequacy of control of RSS-augmented configurations was evaluated in fixed-base simulation by five pilots using the Cooper-Harper rating scale.[3] In order to insure feasibility of design implementation, all sensors were to be integral to the aircraft, and feedback electronic compensation sufficiently simple to permit analog mechanization. Since analysis and synthesis of the RSS was to be based on use of linearized, rigid-body equations of motion, all RSS control surface activity was constrained to the linear range. Undetected failure of the most critical feedback loop of either the longitudinal or lateral RSS was to have no detrimental effect on aircraft handling qualities. Finally, this study culminated in limited flight testing of the prototype longitudinal and lateral RSS's aboard the NASA general purpose airborne simulator (GPAS). GPAS is a modified Lockheed JetStar, equipped with both conventional and direct lift and side force control surfaces, an onboard analog computer, an extensive sensor array, and a complete flight data acquisition system.

II. Synthesis and Analysis

For low-level flight, there is a 1% probability that, once turbulence is encountered, a root-mean-square vertical gust velocity w_g of 2.1 m/sec (7 fps) will be exceeded. The prototype RSS's were designed to operate at this level of turbulence. A 99% probability that control surfaces commanded by the RSS will not saturate is guaranteed by restricting their root-mean-square excursions in response to the design turbulence level to 38% of the available range. Initial design studies were restricted to the GPAS aircraft flying at low altitude in the approach configuration; the instrument landing system (ILS) task being most amenable for critical pilot evaluation of handling qualities.

A basic longitudinal RSS is shown in block diagram form in Fig. 2. Here true vertical acceleration, as measured at the aircraft center of gravity, is fed back to the direct lift flaps through a pure gain K_{a_z} (essential feedback). Perturbation pitch attitude is fed back to the elevator through a pure gain K_θ (auxiliary feedback). The necessity for the auxiliary feedback is apparent from Fig. 3, a root locus diagram depicting the effect of the feedback on the RSS-augmented aircraft short period and phugoid modes. As K_{a_z} is increased, the short period natural frequency ($\omega_{n_{sp}}$) is reduced. Feedback of pitch attitude restores $\omega_{n_{sp}}$ and stabilizes the phugoid mode. Moderate values of K_θ also serve to improve system performance in terms of reduction of σ_{a_z}, root-mean-square vertical acceleration response to turbulence (Fig. 4).

Additional insight into the mechanisms affecting longitudinal RSS performance can be gained by examining a simplified expression for σ_{a_z} due to turbulence.[4] The following assumptions have been made in the derivation: turbulence is represented as white noise passed through a first-order filter, effect of pitch gust is negligible, surface actuators are perfect, and effect of phugoid dynamics is negligible. If only the highest-order terms (based on GPAS aerodynamics)

Table 1 Characteristics of longitudinal ride smoothing systems

	Basic JetStar	Longitudinal RSS I	Longitudinal RSS II
ζ_{sp}	0.546	0.567	0.534
$\omega_{n_{sp}}$	0.266 Hz	0.356 Hz	0.312 Hz
ζ_{ph}	0.054	0.522	0.158
P_{ph}	36.6 sec	53.2 sec	52.9 sec
$T_{\frac{1}{2}ph}$	74.8 sec	9.6 sec	36.8 sec
n/α	6.22 g/rad	6.22 g/rad	4.03 g/rad
σ_{a_z}	0.1178 g	0.0572 g	0.0607 g
σ_{a_x}	0.0112 g	0.0040 g	0.00454 g
σ_{δ_f}	--	9.7°	12.2°
σ_{δ_e}	--	0.4°	0.4°
% reduction σ_{a_z}	--	51.8%	49.4%
% reduction σ_{a_x}	--	64.6%	59.5%

in each power of the Laplace variable are retained, one finds that

$$\sigma_{a_z} \propto \frac{K_{st}}{\omega_{n_{sp}}^2}\left\{\frac{(K_\theta M_{\delta_e})^2}{\omega_0}+\frac{\pi}{4\sigma_{sp}}\left[(K_\theta M_{\delta_e})^2(4\zeta_{sp}^2-1)-\omega_{n_{sp}}^2(\omega_{n_{sp}}^2+M_q{}^2+2K_\theta M_{\delta_e})\right]\right\}^{1/2} \quad (2)$$

where

$$K_{st} \equiv Z_w/(1-K_{a_z}Z_{\delta_f}) \quad (3)$$

$$-2\sigma_{sp}=2\zeta_{sp}\omega_{n_{sp}} \cong -M_q-K_{st} \quad (4)$$

$$\omega_{n_{sp}}^2 \cong -U_0M_w-K_\theta M_{\delta_e}+K_{st}(M_q-K_{a_z}U_0M_{\delta_f}) \quad (5)$$

and ω_0 is the lower limit for a truncated input turbulence (white noise) power spectra. The stability derivatives are in dimensional form and are taken with respect to body reference (nonstability) axes.[5] The dominant factors in the expression for σ_{a_z} are K_{st} and $\omega_{n_{sp}}$. The static gain K_{st} is simply the ratio of the lift curve slope Z_w to an expression involving the direct lift flap effectiveness Z_{δ_f}, multiplied by the vertical acceleration feedback gain. Since $Z_{\delta_f}<0$, increasing K_{a_z} essentially results in a reduction in the effective aircraft lift curve slope. The reduction in σ_{a_z} with increasing $\omega_{n_{sp}}$ also is an intuitively obvious result. The input power spectra (filtered white noise) decays at a rate of 40 dB/decade; thus, the higher the aircraft effective short-period resonant frequency, the lower the magnitude of response to turbulence. The slight degradation in system performance at high values of K_θ is caused by the damping ratio ζ_{sp} falling below $\zeta_{sp}=0.5$ (second term inside the radical). The accuracy to which this simplified analytic expression predicts system performance is shown graphically in Fig. 5. The surface marked "digital" represents computer-generated contours with no approximations.

Considerable improvement in both the acceleration alleviation performance and closed-loop system dynamics was achieved by including simple analog-compensating circuits in both the acceleration and pitch attitude feedback paths. The resulting control system, designated longitudinal RSS I, is depicted in block diagram form in Fig. 6. Of particular importance from the control viewpoint is the inclusion of the "washout" filter $[s/(s+1)]$ in the acceleration feedback loop. By exponentially decaying the acceleration feedback signal, this filter permits the pilot to command long-term normal acceleration changes in a conventional manner (n/α parameter unaffected). A performance surface, similar to that presented for the baseline longitudinal RSS, is shown for longitudinal RSS I, as Fig. 7. Note that the magnitude of the acceleration feedback gain K_{a_z} is restricted by the condition that the direct lift flap activity at the design turbulence level be restricted to $\sigma_{\delta_f}=10°$ by linearity considerations. Also indicated are lines of constant short period damping ratio ζ_{sp} and natural frequency $\omega_{n_{sp}}$. The system design point was chosen to take full advantage of direct lift flap effectiveness; both $\omega_{n_{sp}}$ and ζ_{sp} are higher than for the basic aircraft at the approach flight condition. A power spectral density plot comparing the response of the basic and longitudinal RSS I-augmented GPAS is presented in Fig. 8. The effectiveness of the RSS is clearly evident in the range of frequencies at and above the aircraft short period resonance peak, as well as in the phugoid range.

An alternate RSS mechanization, designated longitudinal RSS II, also was developed. It differs from the previous system only in the form of the acceleration feedback loop compensation, which uses a filter to attenuate the signal at the phugoid frequency. Although almost equivalent to longitudinal RSS I in terms of performance, this system has a slight adverse effect on the control parameter n/α.

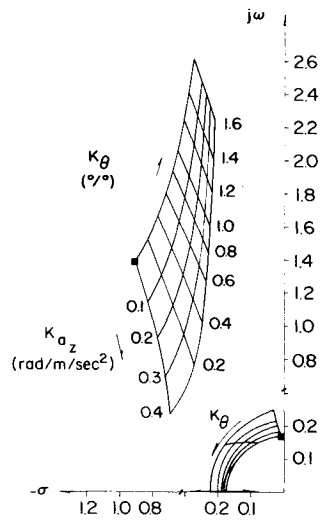

Fig. 3 Root locus for basic longitudinal RSS.

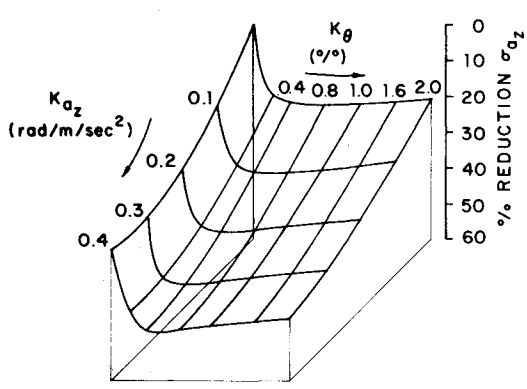

Fig. 4 Performance of basic longitudinal RSS; σ_{a_z} as a function of K_{a_z} and $K\theta$.

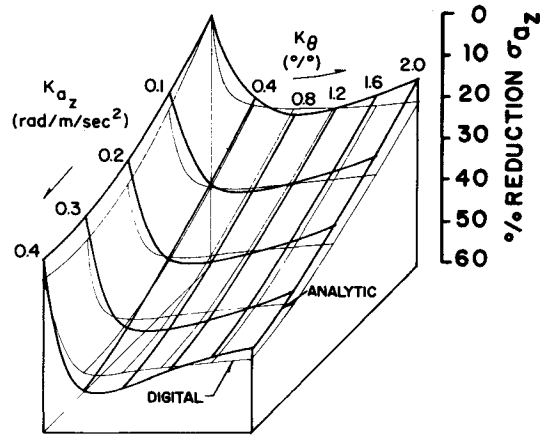

Fig. 5 Comparison of digitally calculated σ_{a_z} with analytic expression.

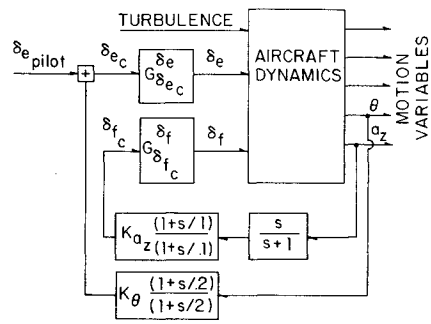

Fig. 6 Longitudinal ride smoothing system I (design point: $K_{a_z}=3.3$ rad/m/sec^2, $K_\theta=0.14$ deg/deg).

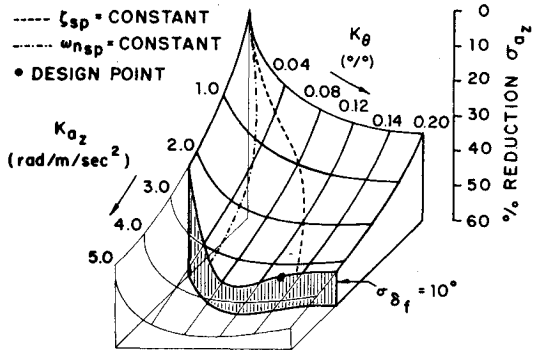

Fig. 7 Performance of longitudinal RSS I; σ_{a_z} as a constrained function of K_{a_z} and $K\theta$.

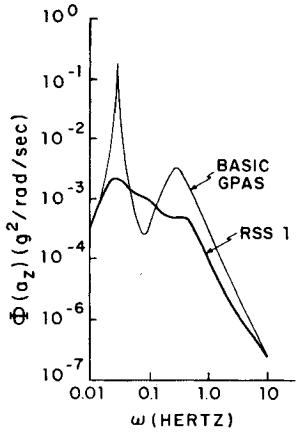

Fig. 8 Comparison of a_z power spectra for basic and longitudinal RSS I-augmented JetStar.

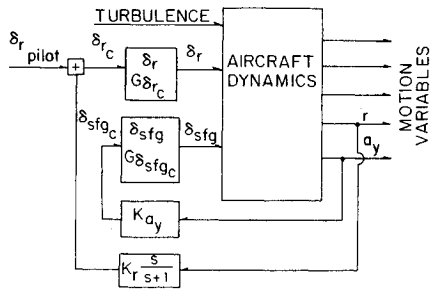

Fig. 9 Lateral ride smoothing system (design point: $K_{a_y} = -3.3$ rad/m/sec^2, $K_r = 1$ deg/deg/sec).

Theoretically predicted longitudinal RSS characteristics are summarized in Table 1.

The prototype lateral RSS, designed to the same specifications as the longitudinal systems, is shown in block diagram form in Fig. 9. As in the longitudinal case, the essential feedback is transverse-acceleration measured at the center of gravity, and the primary control surfaces are direct side force generators. Since this loop closure tended to destabilize the Dutch roll mode, a conventional yaw damper also was incorporated. The performance of the lateral RSS is depicted as the function of a feedback gains in Fig. 10. The surface activity constraint $\sigma_{\delta_{sfg}} < 10°$ is less important in this case than the handling qualities criterion[2] that $(\zeta\omega_n)_{dr} \geq 0.15$. Attenuation of acceleration response to turbulence is achieved for most frequencies below approximately 2 Hz. A summary of lateral RSS characteristics at the selected design point is given in Table 2.

An analytic expression for lateral acceleration response to turbulence with the RSS engaged also was derived.[4] The following simplifying assumptions were made: β_g was represented as white noise passed through a first-order filter, r_g and p_g were neglected, the spiral mode root was set equal to

Table 2 Characteristics of lateral ride smoothing systems

	Basic JetStar	Lateral RSS
ζ_{dr}	0.045	0.155
$\omega_{n_{dr}}$	1.36 rad/sec	1.195 rad/sec
τ_R	0.87 sec	0.61 sec
$T_{\frac{1}{2}_R}$	0.61 sec	0.42 sec
$T_{\frac{1}{2}_s}(T_2)_s$	418 sec	(37.5) sec
σ_{a_y}	0.0312 g	0.0047 g
σ_r	2.35°/sec	1.56°/sec
σ_p	5.01°/sec	1.95°/sec
$\sigma_{\delta_{sfg}}$	--	7.8°
σ_{δ_r}	--	0.92°
% reduction σ_{a_y}	--	84.5%
% reduction σ_r	--	43.5%
% reduction σ_p	--	61.0%

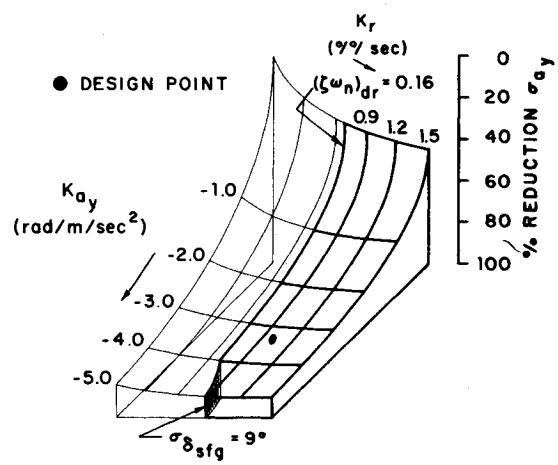

Fig. 10 Performance of lateral RSS; σ_{a_y} as a constrained function of K_{a_y} and K_r.

zero, and all actuators are perfect. For a yaw damper with a 1-sec washout time constant, the following expression for root-mean-square transverse acceleration results:

$$\sigma_{a_y} \propto \frac{K_{s_1}'^2}{(R^2+\omega_{n_{dr}}^2)-4R^2\sigma_{dr}^2}\cdot\left\{R(R^2-L_p'^2)+\frac{1}{2\sigma_{dr}}\left[(\omega_{n_{dr}}^2+R^2)(\omega_{n_{dr}}^2-L_p'^2)+R^2 2\omega_{n_{dr}}^2(2\zeta_{dr}^2-1)\right]\right\}^{1/2} \tag{6}$$

where

$$K_{st}' \equiv \frac{V_{T_0}Y_v}{(1+K_{a_y}Y_{\delta_{sfg}})} \tag{7}$$

$$\omega_{n_{dr}}^2 \cong L_p'N_r' - N_p'L_r' + \cos\theta_0 N_\beta' - \sin\theta_0 L_\beta' \tag{8}$$

$$-2\sigma_{dr} = 2\zeta_{dr}\omega_{n_{dr}} \cong Y_v - K_r N_{\delta_r}'\cdot f \tag{9}$$

$$R \cong -L_p - N_r - K_r N_{\delta_r}(1-f) + Y_v - \frac{Y_v - K_{a_y}K_r N_{\delta_{sfg}}' Y_{\delta_r}}{(1+K_{a_y}Y_{\delta_{sfg}})} \tag{10}$$

and f was determined empirically to be 0.375. The factor f is numerically equivalent to the ratio of the transfer functions

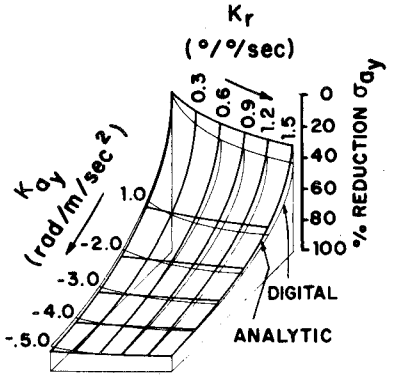

Fig. 11 Comparison of digitally calculated σ_{a_y} with analytic expression.

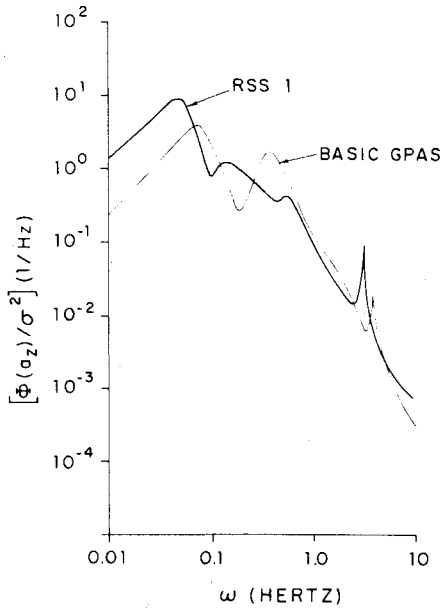

Fig. 12 Comparison of a_z power spectra for basic and longitudinal RSS I-augmented JetStar (flight data).

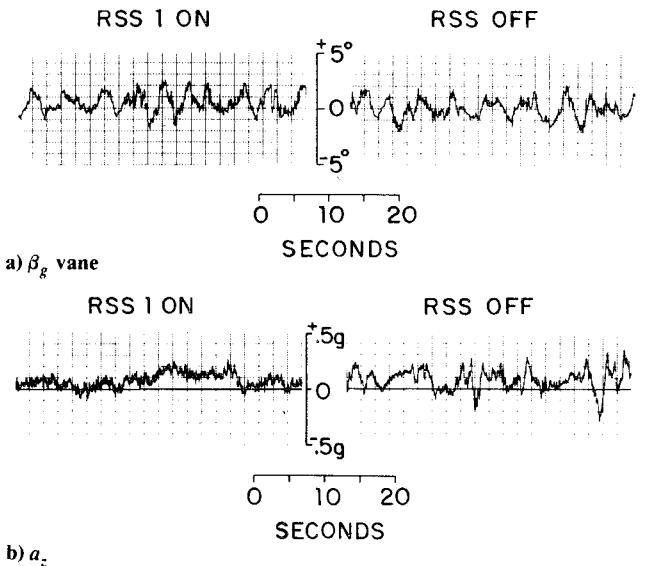

Fig. 13 Time history; basic and longitudinal RSS I-augmented JetStar in turbulence (flight data).

Table 3 Predictions of comfort model

	Comfort rating	% passengers satisfied with ride quality
Basic GPAS	3.6	63
Longitudinal RSS I and lateral RSS	2.7	86
Longitudinal RSS II and lateral RSS	2.8	84

G'_Λ and G^p_Λ at steady state, and essentially prorates the yaw damper effectiveness between the roll subsidence and Dutch roll modes. Although Eq. (6) appears rather formidable, the dominant term is the expression outside the brackets. This term is analogous to that found in the expression for $\sigma_{a_z} \cdot K'_{st}$, the static gain, is reduced as the feedback gain K_{a_y} is increased ($Y_{\delta_{sfg}} > 0$). Response also is attenuated as the frequency of the Dutch roll mode $\omega_{n_{dr}}$ or the magnitude of the roll subsidence root R are increased. Agreement between the analytically predicted performance and the more exact digital calculation is excellent for values of K_{a_y} in the region of interest (Fig. 11).

The prototype longitudinal and lateral ride smoothing systems, as described, meet all of the conditions for successful design as stated previously, with the possible exception of the failure mode criterion. The required system command signals are readily available from typical aircraft instruments. The equalization circuits are mechanized easily. Minimal handling qualities specifications would appear to be satisfied. But what of the passenger and his comfort? For locations at or near the aircraft center of gravity, at the design turbulence condition, the comfort model predictions are shown in Table 3. Only the relatively small size of the GPAS direct lift flaps prevents an even more substantial improvement in ride quality.

III. Simulation Experiments

Five pilots participated in a simulator evaluation of the RSS effect on aircraft handling qualities. These experiments were conducted with the NASA Flight Research Center fixed-base, hybrid computer-controlled, transport aircraft simulator. During runs in simulated atmospheric turbulence, only three disturbance components, w_g, r_g, and p_g, were introduced. The level of simulated turbulence was maintained somewhat below the design level so as not to mask subtle differences in handling qualities between various configurations.

Four precision tasks were flown by all of the pilots. The first, a longitudinal control problem, was defined as a 1-min 1000-ft (305 m) climb, 30-sec stabilization period, and 1-min, 1000-ft descent, with heading and airspeed to be held constant. The lateral task was defined as a 1-min 90°-heading change, 30-sec stabilization, and return to initial heading in 1 min, with altitude and airspeed held constant. The combined-axis task was a superposition of the two previous problems. Finally, the pilots made a simulated 3° ILS approach to a 200-ft (61-m) breakout altitude. The ILS task was initiated with the aircraft on the runway heading at an altitude below the glide slope and offset from the localizer. Failure modes were simulated in the course of the first two problems by opening the pitch attitude/yaw rate feedback loops, without warning, approximately 60 sec after the beginning of a run. Evaluation pilots were asked to comment on, and rate, the various configurations using the Cooper-Harper rating scale.[3] The results of these experiments are summarized in Table 4.

For manuevering flight in smooth air, no substantial change in pilot opinion rating (POR) resulted when the RSS's were engaged. Even in the simulated failure mode cases, the configurations were judged equivalent to the basic aircraft. During the simulated ILS approach, however, all of the pilots reported a significant decrease in workload. In the longitudinal axis, the average ratings indicate that the RSS-augmented aircraft is equivalent to the basic GPAS in smooth air. Failure modes proved to result in a configuration no worse than the original aircraft.

Table 4 Average pilot opinion ratings (Cooper-Harper scale)

		Rating	Standard Deviation
Longitudinal Task	Basic Aircraft	2.4	0.3
	Longitudinal System I On	2.5	0.5
	Longitudinal System II On	2.1	0.2
	Longitudinal System I On - θ Loop Failed	2.3	0.2
	Longitudinal System II On - θ Loop Failed	2.7	0.3
Lateral Task	Basic Aircraft	3.1	0.8
	Lateral System On	2.5	0.5
	Lateral System On - r Loop Failed	3.0	0.4
Combined Axis Task	Basic Aircraft	3.1	0.7
	Longitudinal System I & Lateral System On	2.5	0.5
	Longitudinal System II & Lateral System On	2.9	0.6

		Longitudinal		Lateral	
		Rating	Standard Deviation	Rating	Standard Deviation
3° ILS Tracking Task	Smooth Air				
	Basic Aircraft	3.2	0.3	2.6	0.4
	Turbulent Air, $\sigma \cong 4$ ft/sec				
	Basic Aircraft	4.3	0.9	5.5	1.4
	Longitudinal System I & Lateral System On	2.8	0.9	3.1	1.7
	Longitudinal System II & Lateral System on	2.9	0.7	3.6	2.3

Table 5 Ride smoothing system flight test results

	Longitudinal RSS I		
	Baseline	Partial Gain	Nominal Gain
σ_{a_z}	0.1047 (0.1178) g	0.0788 (0.0794) g	0.0518 (0.0572) g
σ_q	0.933 (1.440) °/sec	0.599 (1.12) °/sec	0.402 (0.700) °/sec
σ_{δ_f}	--	5.31 (5.95) °	7.70 (9.90) °
% reduction σ_{a_z}	--	24.7 (32.6) %	50.5 (51.8) %
% reduction σ_q	--	35.8 (22.3) %	56.9 (51.3) %

	Lateral RSS	
	Baseline	Partial Gain
σ_{a_y}	0.0307 (0.0350) g	0.0206 (0.0158) g
σ_r	1.32 (2.35) °/sec	0.88 (1.65) °/sec
$\sigma_{\delta_{sfg}}$	--	2.14 (2.67) °/sec
% reduction σ_{a_y}	--	32.9 (54.9) %
% reduction σ_r	--	33.0 (30.0) %

IV. Flight Tests

Only two RSS evaluation flights were made before unrelated hardware problems curtailed the experiments. Although the data generated were thus insufficient for high statistical confidence, the observed trends were most encouraging.

Of the two prototype longitudinal systems, only RSS I was tested in flight. In addition to baseline data, measurements were made with the system operating at part gain and nominal feedback gain levels. The lateral RSS was tested at the nominal yaw damper gain, but GPAS hardware problems prevented operation at more than 15% of the design acceleration feedback level. The results of these flight tests are summarized in Table 5. The experimental values have been scaled linearly to the design turbulence level. Corresponding theoretically calculated values are indicated in parentheses.

The agreement between theoretical and measured accelerations for the baseline cases is quite good. The theoretical calculations, however, significantly overestimate aircraft response in pitch rate and yaw rate. The measured per-

formance of longitudinal RSS I, in terms of percent reduction in σ_{a_z} and σ_q at the design feedback levels, is in excellent agreement with predicted performance. The acceleration alleviation provided by the lateral RSS, however, is significantly below the anticipated level, while the reduction of σ_r is very close to the predicted value. Had the acceleration feedback loop been open, the yaw damper alone would have provided a 38.3% reduction in σ_{a_y} and a 29.0% reduction in σ_r. Thus, it would appear that the side force generators provided no measureable benefit at the very low levels of K_{a_y} attainable in these tests.

A normalized comparative power spectral density plot of the output of the center of gravity normal accelerometer for the baseline and longitudinal RSS I nominal gain cases is shown in Fig. 12.

Since the areas under both curves are identical, the plot displays only the relative RSS effectiveness of particular frequencies. The greatest acceleration alleviation can be seen to occur from frequencies somewhat below the short period peak to approximately 1 Hz. This conclusion is in clear agreement with the theoretical predictions (Fig. 8). The sharp spikes in the experimental curves occurring at 3 to 4 Hz are attributable to resonance of the accelerometer mounting plate.

The qualitative behavior of longitudinal RSS I operating at nominal gains is shown in Fig. 13. The turbulence field, as indicated by the β_g vane excursions, is approximately equivalent for both records; the aircraft response, however, is clearly attenuated with the RSS engaged.

V. Conclusions

Although the GPAS aircraft is not a STOL-class aircraft, the simple ride smoothing systems described previously, when integrated with conventional stability augmentation systems, can be implemented successfully.[4] Such systems will not only improve ride qualities and passenger acceptance significantly, but also will reduce pilot workload during precision flight in turbulence. Analytic models can be generated to determine sensitivity and quantitative information during the design phase.

Acknowledgment

This work was sponsored by NASA Flight Research Center through Grant No. NGR 47-005-202.

References

[1] Jacobson, I. D. and Richards, L. G., "Ride Quality Evaluation II: Modelling of Airline Passenger Comfort," *Ergonomics*, Vol. 19, No. 1, 1976, pp. 1-10.

[2] Anonymous, "Military Specifications – Flying Qualities of Piloted Airplanes," MIL-F-8785B, Aug. 7, 1969.

[3] Cooper, G. E. and Harper, R. P. Jr., "The Use of Pilot Rating in the Evaluation of Aircraft Handling Qualities," NASA TN D-5153, April 1969.

[4] Lapins, M., "Application of Active Controls Technology to Aircraft Ride Smoothing Systems," Ph.D. Dissertation, University of Virginia, May 1975; also NASA CR 145980, May 1975.

[5] McRuer, D., Ashkenas, I., and Graham, D., "Vehicle Equations of Motion," in *Aircraft Dynamics and Automatic Control*, Naval Air Systems Command, Department of the Navy, Washington, D. C., Aug. 1968, Chap. 4.